Supplemental File

Romano, Seu, et al.

Erythroblastic islands foster granulopoiesis in parallel to terminal erythropoiesis

Supplemental Materials and Methods

Mice

All mouse use was approved by the Institutional Animal Care and Use Committee (IACUC) at Cincinnati Children's Hospital Medical Center and at the Feinstein Institutes for Medical Research. Male or female wild-type (WT) C57BL/6J mice aged 3-6mo were used for all experiments unless otherwise specified. Gfi1$^{-/-}$ and Gfi1$^{+/-}$ littermates were used at 8-9 weeks of age due to decreased survival of Gfi1$^{-/-}$ mice.[1,2] Gfi1$^{+/-}$ littermates appear normal and are used as an age-appropriate littermate control.[1,2] For collagen induced arthritis (CIA), DBA1/J mice were subjected to CIA according to standard protocol.[3] Bone marrow from IL10$^{-/-}$ mice (Jackson Labs Stock No. 002251) was harvested upon onset of inflammatory bowel disease symptoms with rectal prolapse. The cecal ligation and peritonitis (CLP) model was performed as previously described.[4] CBCs were performed prior to harvest to confirm experimental mice had leukocytosis. CLP and IL10$^{-/-}$ mice also had anemia, as previously described.[5,6] For reconstitution experiments, β1^{glo} mice (Jackson Labs Stock No. 018393) were used in addition to WT.

Imaging flow cytometry (IFC)

For IFC of EBIs, cell clusters in the 3% BSA layer were fixed by adding paraformaldehyde to a final concentration of 4% for 30min and washed with phosphate buffered saline (PBS). Fixed EBI preparations were blocked with anti-FcR (BD Bioscience) for 20 min at room temperature (RT), washed, and, incubated with a cocktail of fluorescently conjugated antibodies including anti-F4/80-AF647 (BM8, Biolegend), anti-CD71-BV421 (RI7217, Biolegend), and CD11b-PE

(M1/70, BD Pharmingen). Samples were incubated at RT for 30min in the dark and then washed with FACS buffer. For nuclear staining, Hoechst 34580 (Sigma) was added with the antibodies and samples were incubated for 1hr at 37°C. Labeled cell clusters were analyzed on an ImageStream^X (ISX-100, Amnis/Luminex) using 40x magnification and analysis was performed in IDEAS analysis software (Amnis) as previously described.[7-9] Briefly, cell clusters are first gated by selecting events with a large area (>300) in the brightfield. These are further refined by selecting for those with expression of both F4/80 and CD71. Lastly, manual inspection and tagging of EBIs is performed, selecting events which possess a central F4/80$^+$ cell with at least 3 adjacent CD71$^+$ cells. In the case of 250µg/kg GCSF treatment which dramatically suppressed medullary erythropoiesis, clusters with three CD71$^+$ cells were rare, owing to the overall paucity of erythroblasts in the bone marrow, so clusters with just two CD71$^+$ cells were considered as EBIs in this analysis. Areas of CD71 and CD11b were determined in the analysis software using the default masks of the appropriate channels.

EBI Reconstitution

To assess non-specific cell interactions, we utilized β1^{glo} mice (Jackson Labs Stock No. 018393) which have widespread expression of EGFP, including expression in hematopoietic cells. WT and GFP$^+$ EBIs and single bone marrow cells were harvested from WT C57BL/6 and β1glo mice. EBIs were collected as described using EBI buffer, while single cells were collected by flushing with IMDM containing 2% FBS in a manner to create a single cell suspension. Combinations of WT and GFP+ EBIs or single cells were mixed 1:1 in excess EBI buffer to mimic the conditions during EBI harvest and incubated for 2 hours. The mixtures were loaded onto BSA gradients and any native and/or reconstituted EBIs were separated by gravity sedimentation, fixed, stained, and evaluated by IFC.

Immunofluorescence Microscopy

Intact pieces of whole bone marrow obtained from flushing the long bones were fixed with 4% PFA for 30 min and deposited onto poly-lysine-coated coverslips. Samples were blocked with PBS + 0.1% Tween-20 + 2% FBS and 2% BSA (blocking buffer) and subsequently incubated with antibodies in blocking buffer diluted 1:1 with PBS overnight at 4°C. After washing, coverslips were mounted (Fluoromount-G, SouthernBiotech) and imaged at 20x and 60x on a Nikon C1 confocal microscope.

Cytospins

EBIs were collected from total bone marrow using gravity sedimentation as described above. Approximately 100,000 cells from the 3% fraction were resuspended in 50uL FBS and cytospun onto poly-lysine (Sigma P4707)-coated cover glass at 400 rpm for 3 minutes. Slides were then stained with hematoxylin and eosin (H&E), mounted, and imaged on a Nikon Ti-E inverted microscope at 60X.

Flow Cytometry

For flow cytometry and sorting of single cells, unfractionated cells and the 3% fraction were dispersed into single cells by washing with PBS and incubating with FACS+10mM EDTA for 15 minutes on ice. Cells were filtered and stained in FACS buffer with appropriate antibodies for 30 minutes at room temperature unless otherwise specified (Supplementary Table 1).
To evaluate erythroblasts, cells were stained with Fixable Viability Dye efllour780 (FVD780, eBioscience), CD45-APC (30-F11, BD Pharmingen), CD44-PerCP Cy5.5 (IM7, BD Pharmingen), Ter119-FITC (TER-119, Biolegend). Analysis was performed as previously described by Liu et al, Blood 2013.[10] To evaluate granulocyte precursors, cells were stained with a biotinylated lineage panel including CD4 (RM4-5, Biolegend), CD8 (53-6.7, Biolegend), CD19 (6D5, Biolegend), B220 (RA3-6B2, BD Pharmingen), Sca1 (D7, Biolegend), and Ter119

(TER119, Biolegend) followed by staining with streptavidin conjugated AF700 (Invitrogen), Fixable Viability Dye eflour780 (eBioscience), cKit-APC (2B8, eBioscience), CD34-PE (RAM34, BD Pharmingen), CD16/32 FcγR-FITC (2.4G2, BD Pharmingen), and Ly6G-BV421 (1A8, Biolegend). Analysis was performed as previously described by Satake et al. J Immunol. 2012.[11] All flow cytometry events were gated on live, single cell events. Unstained and FMO (panels with all fluorescent antibodies minus one) samples were used as negative controls to establish gating (Supplemental Figure 10). All flow cytometry experiments were analyzed on a FACSCanto flow cytometer (BD) and data were analyzed using FlowJo (FlowJo LLC, Ashland, OR, USA).

Fluorescence activated cell sorting (FACS)

EBIs from WT bone marrow were collected by density gradient sedimentation as described above and then dispersed to single cells by incubation in buffer containing EDTA. Bone marrow cells were sequentially gated as displayed in **Supplementary Figure 2** and sorted on a BD FACS Aria II cell sorter. $CD71^+$, $CD11b^+$, and $F4/80^+$ cells were collected.

Single Cell Genomics Analysis

The 10x Genomics libraries were aligned to the mouse genome (mm10) downloaded from ensembl, with unique molecular index (UMI) quantified gene counts obtained using the Cell Ranger workflow using the mm10-2.1.0 reference transcriptome. scRNA-Seq samples (n=5) were sequenced to a depth of 48 to 274 million reads, with a range of 1,330-2,182 for the sorted populations and 3,443-7,715 for the unsorted populations called cell barcodes from each library, and 6,192-8,159 UMI per cell on average. CITE-Seq samples (n=2) were sequenced to a depth of 368 to 385 million reads, with a range of 8,176-8,922 called cell barcodes from each library, and 9,327-9,719 UMI per cell on average. Cell Ranger filtered cellular barcodes were jointly analyzed from A) scRNA-Seq ($CD71^+$, $CD11b^+$, $F4/80^+$, unsorted) and B) CITE-Seq data in

AltAnalyze and ICGS2 (Iterative Clustering and Guide-gene selection version 2) to produce normalized gene counts (counts per ten thousand (CPTT) UMIs) and cell populations.[12] ICGS2 was run on GEX-only profiles following removal of ambient background associated RNAs with SoupX (contamination fraction 15%).[13] ICGS was performed using the software default options and Euclidean clustering, with no forced resolution parameter, in addition to a PageRank down-sampling threshold of 5,000 cells. Cell population names were revised from the original ICGS2 predictions based on the literature (marker gene driven), with an emphasis on prior well-defined hematopoietic lineage notations.[2] The software cellHarmony was used to assign cell population labels for the separate validation unsorted sample based on the centroid-based cell-alignment automated workflow.[14] All scRNA-Seq samples were jointly projected into a common UMAP embedding using the python library scikit-learn to train and transform the ICGS2 marker genes data using PCA (top 50 components), as described for the umap_transform function in the R uwot package.[15] For the CITE-Seq dataset, a comprehensive differential expression and gene regulatory analysis was also performed in the software cellHarmony with cell-to-cluster assignments from the joint ICGS2 analysis of the Saline and Epo samples (option --referenceType None) and an empirical Bayes moderated t-test $p<0.05$, FDR adjusted and fold>1.2. UMAPs colored by marker gene expression and bar chart visualizations were all performed in AltAnalyze.[16] Bubble plots were generated using R ggplot2 package.[17] The scRNA-seq and CITE-seq datasets have been deposited into the Gene Expression Omnibus (accession number pending).

Accumax Dissociation

Accumax solution (Invitrogen) was thawed and added to cells at a 1:1 ratio with PBS and incubated at 37°C for 10 minutes. Cells were then filtered, counted, and prepared for downstream analysis.

Statistics

Statistical analysis was performed using GraphPad Prism version 9.0.0 for Windows, GraphPad Software, San Diego, California USA, **www.graphpad.com**. Unpaired t-test was used to compare the slopes of $CD11b^+$ versus $CD71^+$ area in EBIs of the different mouse models and erythropoiesis conditions, based on the assumption that these values would be normally distributed about the mean for a given condition. This assumption was supported by kurtosis and skewness measures and a Jarque-Bera test on a set of n=8 slopes for control mice. Unless otherwise noted, we report the mean ± SD for each group and the two-tailed p-value according to an unpaired t-test. Statistical tests was not performed for the comparison of slopes in **Figure 5B,E,&H** where 2 samples for each experimental and each control mouse model of AoI were analyzed.

The ratios for the $CD71^+$ to $CD11b^+$ area of the individual EBIs are not normally distributed, as can be seen in the violin plots in **Figures 4C&F, 5C,F,I,** and **6D**, so we used a non-parametric test (Mann-Whitney) for statistical analysis of this data. For CD11b:CD71 ratio tests, we report the median for each group and the p-value according to Mann-Whitney test. For correlation coefficient values, we report the Spearman's r and corresponding p value. Significance was set at $p < 0.05$.

Study Approvals

This work was approved by Cincinnati Children's Hospital Medical Center IACUC (2020-0041) and Feinstein Institutes IACUC (2018-009, 2019-009).

	Conjugate	Manufacturer	Catalog No.	Used for:
Imagestream/IF				
F4/80	AF647	Biolegend	123122	Imagestream, IF
CD11b	PE	BD Pharmingen	557397	Imagestream, IF
CD11b	APC-Cy7	Biolegend	101226	Imagestream
CD11b	PB	Biolegend	101224	Imagestream
CD71	FITC	BD Pharmingen	553266	Imagestream
CD71	BV421	Biolegend	113813	Imagestream, IF
CD71	PE	BD Pharmingen	553267	Imagestream
Hoechst 34580		Sigma	63493	Imagestream
Ly6C	AF488	Biolegend	128022	Imagestream
Flow Cytometry				
Fixable Viability Dye	eFlour780	eBioscience	65-0865-14	Erythroblast, Gran Precursor Flow
CD45	APC	BD Pharmingen	559864	Erythroblast Flow
CD44	PerCp Cy5.5	BD Pharmingen	560570	Erythroblast Flow
Ter119	FITC	BD Pharmingen	557915	Erythroblast Flow
CD4	Biotin	Biolegend	100508	Gran Precursor Flow
CD8	Biotin	Biolegend	100704	Gran Precursor Flow
CD19	Biotin	Biolegend	115504	Gran Precursor Flow
B220	Biotin	BD Pharmingen	51-01122J	Gran Precursor Flow
Sca1	Biotin	Biolegend	108104	Gran Precursor Flow
Ter119	Biotin	BD Pharmingen	51-09082J	Gran Precursor Flow
Streptavidin	AF700	Invitrogen	S21383	Gran Precursor Flow
cKit	APC	eBioscience	17-1171-82	Gran Precursor Flow
CD34	PE	BD Pharmingen	551387	Gran Precursor Flow
FcGR 16/32	FITC	BD Pharmingen	553144	Gran Precursor Flow
Ly6G	BV421	Biolegend	127628	Gran Precursor Flow, Imagestream
MACS				
cKit	Biotin	Biolegend	105804	
Ly6G	Biotin	Biolegend	127604	
SiglecF	Biotin	Biolegend	155512	
CD3e	Biotin	BD Pharmingen	51-01082J	
Ter119	Biotin	Biolegend	116204	

Supplemental Table 1.

References

1. Hock H, Hamblen MJ, Rooke HM, et al. Intrinsic Requirement for Zinc Finger Transcription Factor Gfi-1 in Neutrophil Differentiation. *Immunity*. 2003/01/01/ 2003;18(1):109-120. doi:https://doi.org/10.1016/S1074-7613(02)00501-0
2. Muench DE, Olsson A, Ferchen K, et al. Mouse models of neutropenia reveal progenitor-stage-specific defects. *Nature*. Jun 2020;582(7810):109-114. doi:10.1038/s41586-020-2227-7
3. Thornton S, Strait RT. Head-to-head comparison of protocol modifications for the generation of collagen-induced arthritis in a specific-pathogen free facility using DBA/1 mice. *Biotechniques*. 2016;60(3):119-28. doi:10.2144/000114388
4. Valdes-Ferrer SI, Papoin J, Dancho ME, et al. HMGB1 Mediates Anemia of Inflammation in Murine Sepsis Survivors. *Mol Med*. May 2016;21(1):951-958. doi:10.2119/molmed.2015.00243
5. Valdes-Ferrer SI, Papoin J, Dancho ME, et al. HMGB1 mediates anemia of inflammation in murine sepsis survivors. *Mol Med*. Dec 29 2015;doi:10.2119/molmed.2015.00243
6. Kuhn R, Lohler J, Rennick D, Rajewsky K, Muller W. Interleukin-10-deficient mice develop chronic enterocolitis. *Cell*. Oct 22 1993;75(2):263-74. doi:10.1016/0092-8674(93)80068-p
7. Seu KG, Papoin J, Fessler R, et al. Unraveling Macrophage Heterogeneity in Erythroblastic Islands. *Front Immunol*. 2017;8:1140. doi:10.3389/fimmu.2017.01140
8. Li W, Wang Y, Zhao H, et al. Identification and transcriptome analysis of erythroblastic island macrophages. *Blood*. Aug 1 2019;134(5):480-491. doi:10.1182/blood.2019000430
9. Tay J, Bisht K, McGirr C, et al. Imaging flow cytometry reveals that granulocyte colony-stimulating factor treatment causes loss of erythroblastic islands in the mouse bone marrow. *Exp Hematol*. Feb 2020;82:33-42. doi:10.1016/j.exphem.2020.02.003
10. Liu J, Zhang J, Ginzburg Y, et al. Quantitative analysis of murine terminal erythroid differentiation in vivo: novel method to study normal and disordered erythropoiesis. *Blood*. Feb 21 2013;121(8):e43-9. doi:10.1182/blood-2012-09-456079
11. Satake S, Hirai H, Hayashi Y, et al. C/EBPbeta is involved in the amplification of early granulocyte precursors during candidemia-induced "emergency" granulopoiesis. *J Immunol*. Nov 1 2012;189(9):4546-55. doi:10.4049/jimmunol.1103007
12. Venkatasubramanian M, Chetal K, Schnell DJ, Atluri G, Salomonis N. Resolving single-cell heterogeneity from hundreds of thousands of cells through sequential hybrid clustering and NMF. *Bioinformatics*. Jun 1 2020;36(12):3773-3780. doi:10.1093/bioinformatics/btaa201
13. Young MD, Behjati S. SoupX removes ambient RNA contamination from droplet-based single-cell RNA sequencing data. *Gigascience*. Dec 26 2020;9(12)doi:10.1093/gigascience/giaa151
14. DePasquale EAK, Schnell D, Dexheimer P, et al. cellHarmony: cell-level matching and holistic comparison of single-cell transcriptomes. *Nucleic Acids Res*. Dec 2 2019;47(21):e138. doi:10.1093/nar/gkz789
15. *uwot: The Uniform Manifold Approximation and Projection (UMAP) Method for Dimensionality Reduction.* Version 0.1.11. 2021.
16. Emig D, Salomonis N, Baumbach J, Lengauer T, Conklin BR, Albrecht M. AltAnalyze and DomainGraph: analyzing and visualizing exon expression data. *Nucleic Acids Res*. Jul 2010;38(Web Server issue):W755-62. doi:10.1093/nar/gkq405
17. *ggplot2: Elegant Graphics for Data Analysis.* Springer-Verlag; 2016.

SUPPLEMENTAL FIGURES

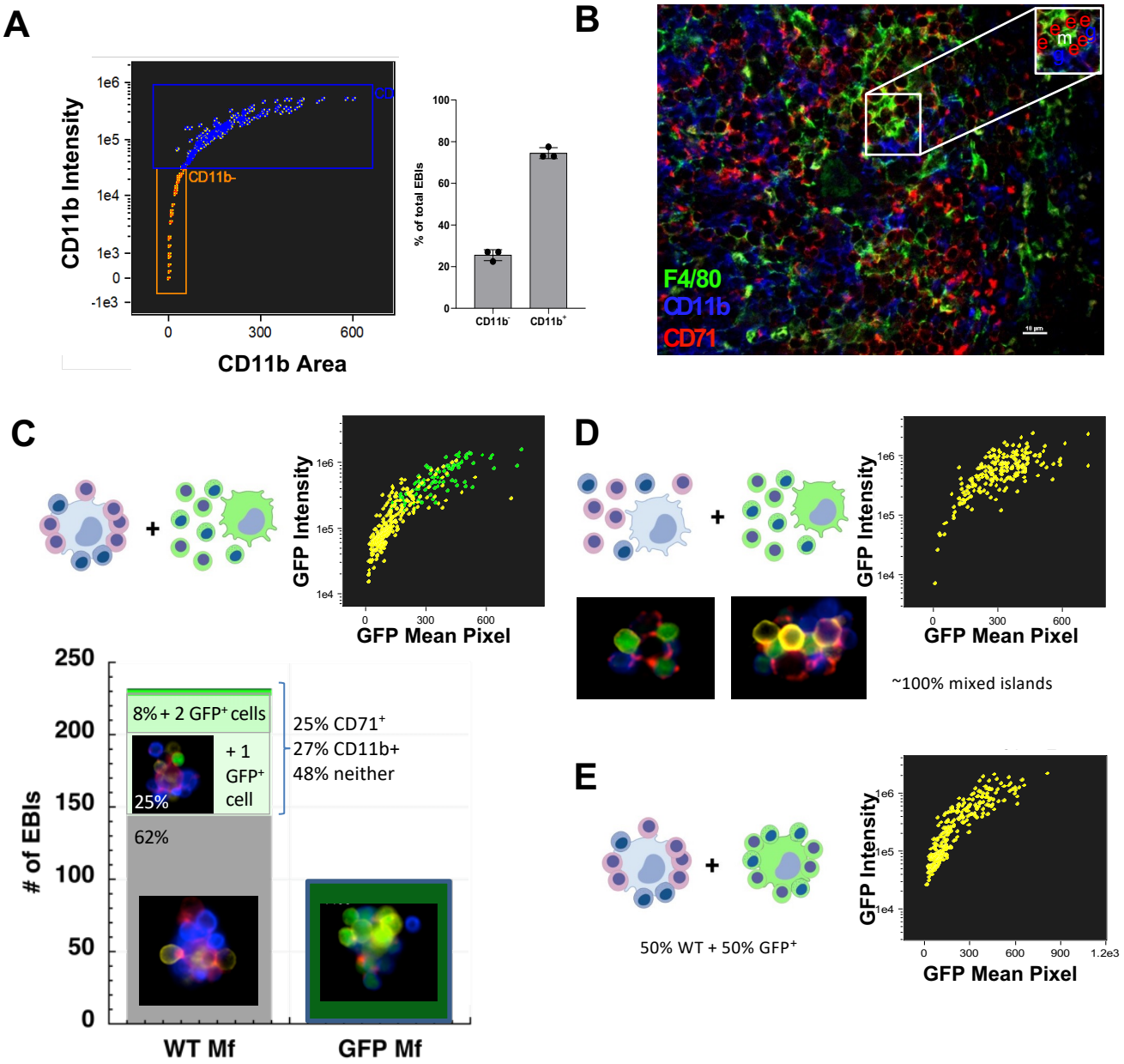

Supplemental Figure 1. CD11b⁺ cells are native component cells of the EBIs and not an artifact created during isolation from the bone marrow. **A.** Representative flow cytogram from IFC demonstrating EBI distribution by area and intensity of CD11b. Most EBIs (~75%) have at least one closely associated CD11b⁺ cell, compared to purely erythroid-constituent EBIs (~25%); bar graph showing mean ± SD from n=3 biologic repeats. **B.** Whole mount immunofluorescence staining of intact bone marrow shows cells stained for CD11b (blue) and CD71 (red) intimately associated with an F4/80⁺ macrophage (green) *in situ*. Inlay is labelled erythroblastic island (e: erythroblast, m: macrophage, g: granulocyte precursor). Scale bar is 10μm. **C.** WT EBIs were mixed with a 10-fold excess of single GFP⁺ bone marrow cells for 2hrs in the same buffer used for EBI harvest and sedimentation, followed by fixation and immunostaining for analysis on the ImageStream. WT EBIs, identified by lack of GFP expression in the central macrophages, were examined for presence of GFP⁺ cells. Whole GFP⁺ EBIs from the donor, that had likely remained intact before mixing, were also observed. **D.** EBIs were isolated from both WT and GFP⁺ mice, as described, and disrupted to single cells by incubation with EDTA. These cells were washed, mixed 1:1 in EBI buffer for 2hrs and then fixed and stained for IFC. The result was 100% mixed EBIs containing both WT (GFP⁻) and GFP⁺ cells. **E.** Isolated, intact EBIs from both WT and GFP mice were mixed at 1:1 ratio for 2hrs and fixed and analyzed from IFC. The result was the preservation of the WT-derived and GFP⁺-derived EBIs, with negligible exchange of cells.

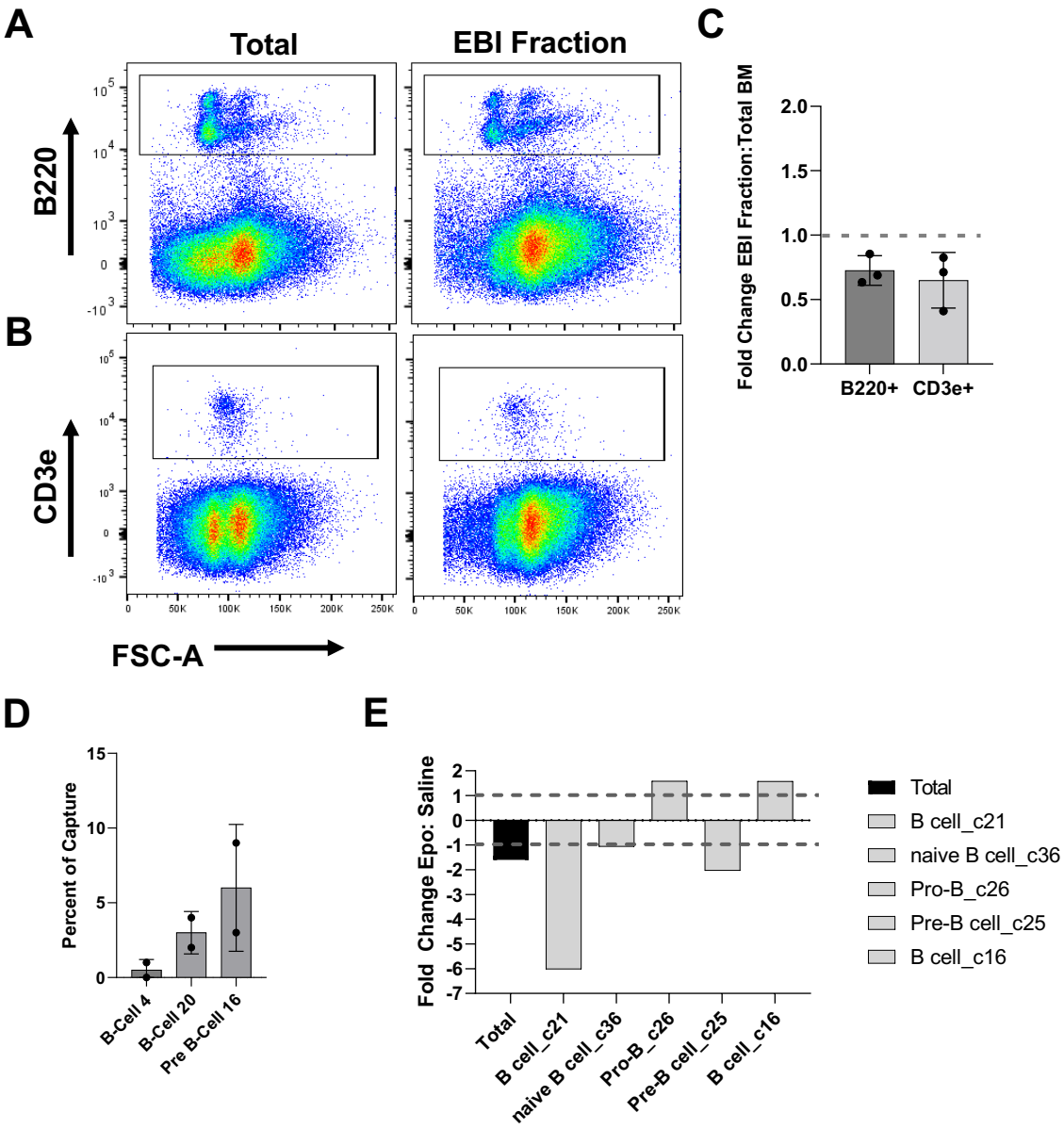

Supplemental Figure 2. B cells and T cells are depleted from the EBI Fraction compared to total bone marrow. Total unfractionated BM and the EBI fraction, after cell dissociation, were evaluated by flow cytometry for B cells or T cells. **A.** Representative flow plots showing the B cells in total unfractionated BM and the EBI fraction. **B.** Representative flow plots showing the T cells in total unfractionated BM and the EBI fraction. **C.** The fold change of each population in the EBI fraction versus the whole BM was calculated in n=3 biologic repeats (fold change is shown as mean ± SD). **D.** From unsorted WT1 and WT2 scRNA-seq captures of EBI component cells, B cells comprise an average of <10% of the total capture. **E.** Fold change in percent of capture from Epo vs saline-treated mouse BM cells, enriched in EBI macrophages, shows both increases and decreases in different B cell clusters, with an overall slight decrease in B cell populations.

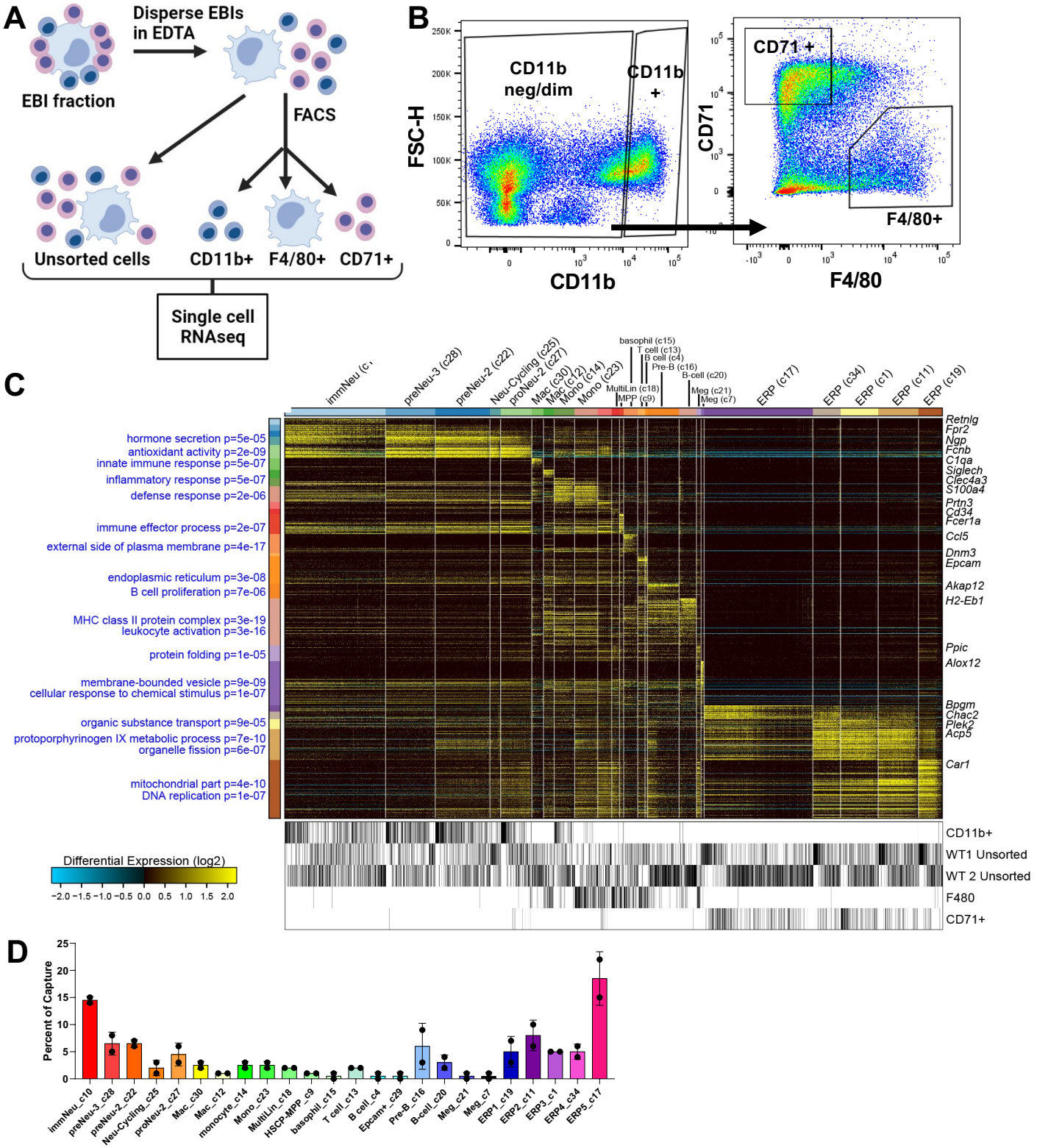

Supplemental Figure 3. Single cell RNA-sequencing (scRNA-seq) analysis of EBI component cells. **A.** Following gradient sedimentation, the EBI clusters were dispersed with EDTA and either were kept unsorted or FACS-sorted for CD11b^{+}, CD71^{+}, and F4/80^{+}/CD11b$^{neg/dim}$ and processed for scRNA-seq. **B.** Flow cytometry gating scheme used to isolate the sorted populations subjected to scRNA-seq. **C.** Heatmap of genes delineated by Iterative Clustering and Guide Gene Selection 2 (ICGS2) in scRNA-seq data (n=17,455 cells). Each black line underneath the heatmap represents a cell within the capture contributing to a given cluster. Relevant ICGS guide genes are displayed on the right and pathways are displayed on the left. **D.** Percent of Capture for unsorted WT1 and WT2, corresponding to comb plot in Figure 3D.

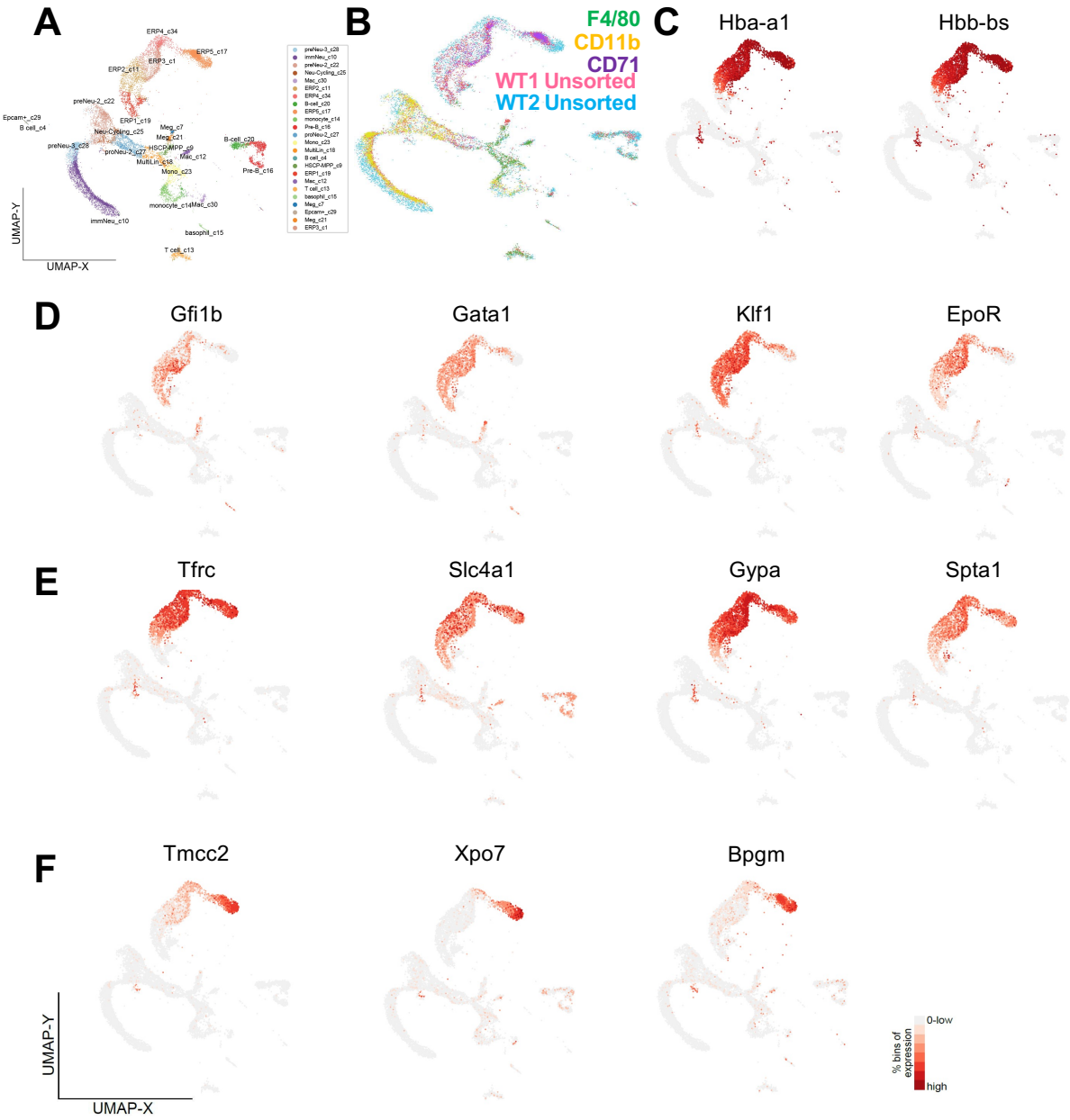

Supplemental Figure 4. Expression of erythroid genes within the scRNAseq UMAP. A, B. UMAP plots showing the different clusters **(A)** and alignment **(B)** of sorted cell populations ($CD71^+$ (purple), $CD11b^+$ (yellow), and $F4/80^+$ (green) populations) with two unsorted samples, as also shown in Figure 3. **C.** Hemoglobin genes are expressed at increasing level in clusters 19 (almost absent), 11, 1, 34, and 17 (most intense), as the erythroblast maturation progresses. **D.** Erythroid transcription factors and erythropoietin receptor (EpoR) are expressed in the same clusters (19, 11, 1, 34, and 17) of the UMAP plot with the gradient of expression level peaking at the clusters 19, 11, and 1. **E.** Transferrin receptor (Tfrc also known as CD71) and red cell membrane protein genes are expressed in clusters 11, 1, 34, and 17. **F.** Genes known to be expressed in the final stages of erythroid maturation in cluster 17.

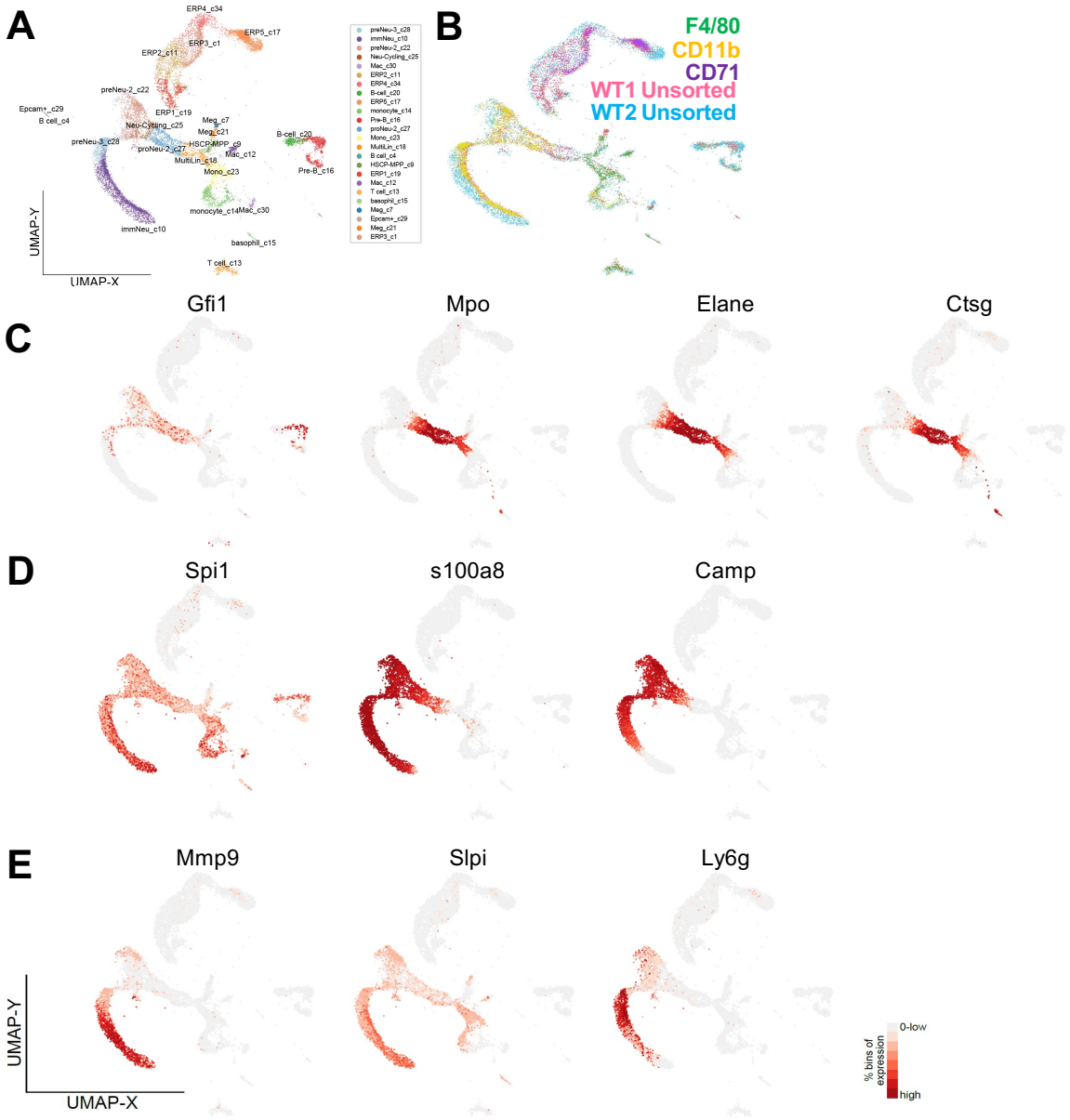

Supplemental Figure 5. Expression of myeloid genes within the scRNAseq UMAP. A, B. UMAP plots showing the different clusters **(A)** and alignment **(B)** of sorted cell populations (CD71$^+$ (purple), CD11b$^+$ (yellow), and F4/80$^+$ (green) populations) with two unsorted samples, as also shown in Figure 3. **C.** Mpo, Elane, and Ctsg are highly expressed in early granulocyte precursors and progenitors in the clusters 27 and 18 within the EBI cells, and Gfi1 highly expressed in early granulocyte precursors proNeu2 (c27). **D.** Intermediate markers of granulocyte maturation can be visualized in the clusters 25, 22, 28, and 10. **E.** Tertiary granule and terminal maturation markers are expressed by cells in populations 28 and 10.

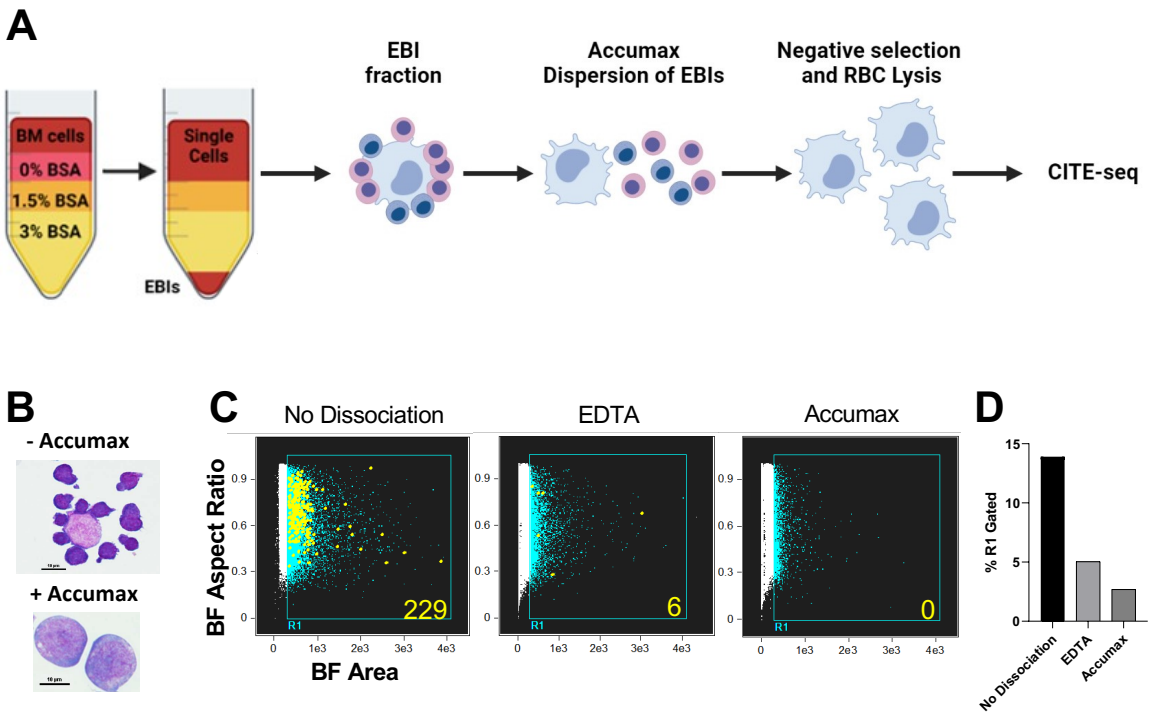

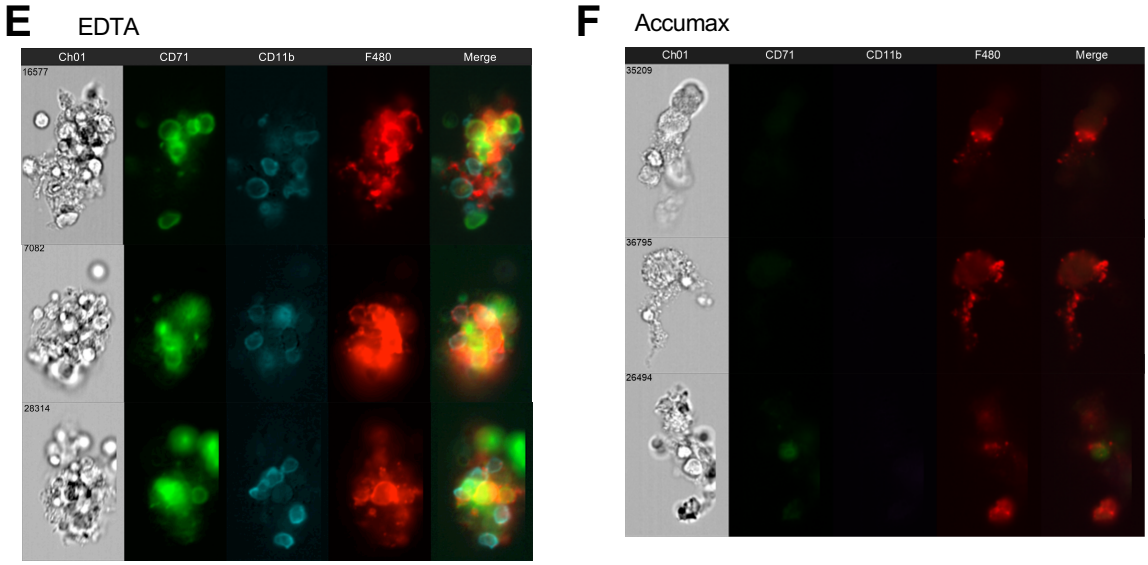

Supplemental Figure 6. Accumax improves dissociation of EBIs to single cells. A. Following gravity sedimentation, the EBI-enriched fraction was dispersed in Accumax followed by red cell lysis and negative selection with antibodies against Ly6G, Cd3e, Siglec F, Ter119, and cKit by AutoMACS. The resulting cell population was subjected to CITE-seq. **B.** Without Accumax dissociation, intact EBIs are observed in Wright-Giemsa-stained cytospins, even after magnetically activated cell sorting (upper image from cytospin of prep without Accumax). After cell separation by Accumax, macrophages without associated erythroblasts (lower image from cytospin of prep with Accumax) were reliably isolated, as described in the methods. **C.** Using Imaging Flow Cytometry, large-sized events are gated in R1. EBIs containing an F4/80+ macrophage and 3 surrounding erythroblasts are marked and quantified in yellow. **D.** The percent of large events gated in R1 decreases with Accumax compared to EDTA dissociation and no dissociation. Representative images of large events in samples treated with EDTA **(E)** or Accumax **(F)**, demonstrating improved dissociation with Accumax.

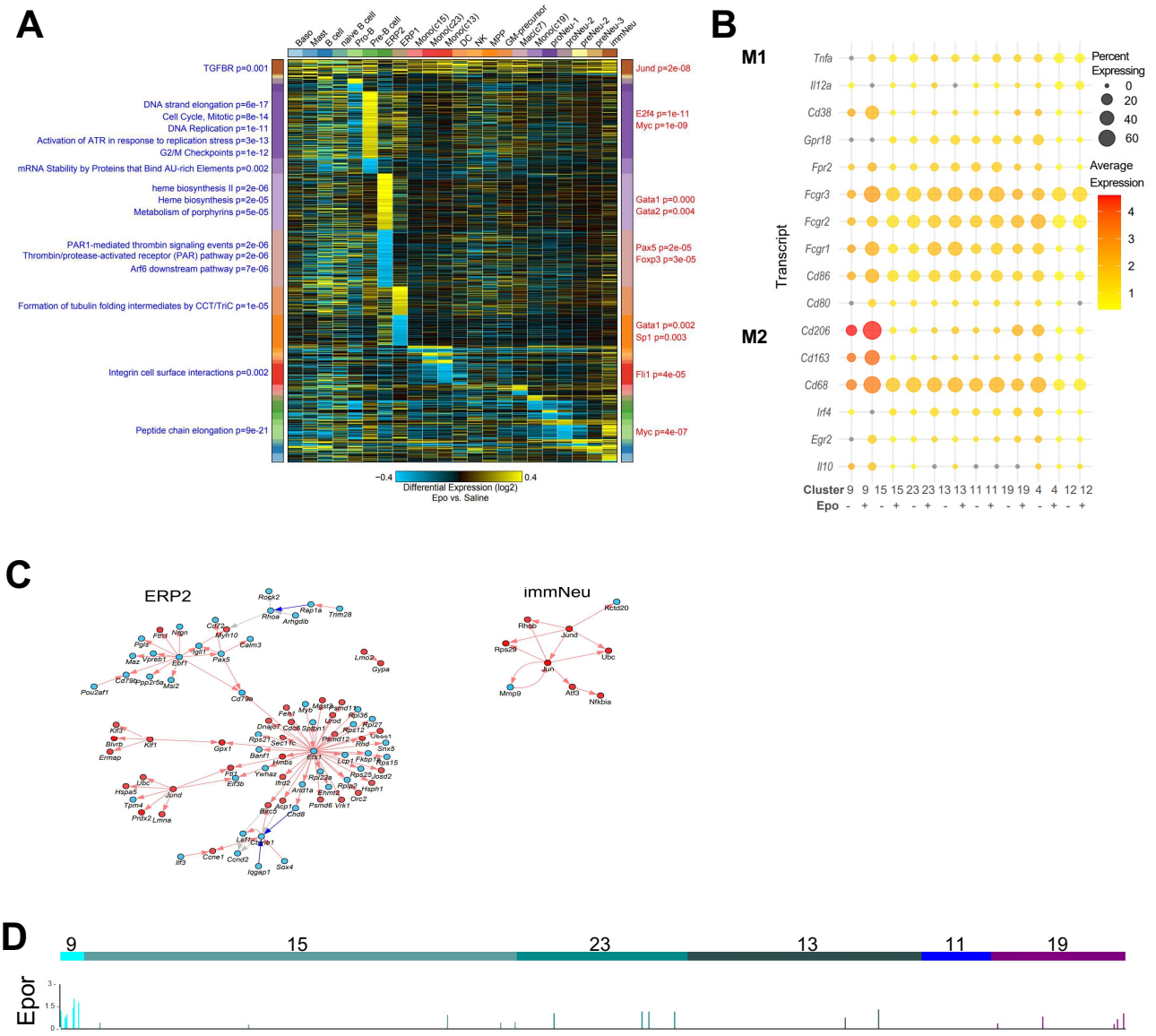

Supplemental Figure 7. Enrichment of EBI macrophages and other component cells for CITE-seq analysis. **A.** Heatmap of differentially expressed transcripts for the different cell groups captured by CITE-seq. Among the two erythroid populations remaining, we observe the predicted regulatory impact following Epo stimulation (Foxp3 versus Gata1 transcriptional repression), upregulated gene expression associated with heme biosynthesis and tubulin formation, and downregulated thrombin signaling, suggesting significant changes in the differentiation kinetics of erythroblast progenitors. **B.** Comprehensive differential expression analyses between Epo stimulated and controls using the software cellHarmony. **C.** A bubble plot showing expression of M1 and M2 markers demonstrates that EBI macrophages have both M1 and M2 characteristics. The size of the bubble indicates the percentage of cells from the total cells within the cluster, including both saline- and Epo treated samples, expressing the gene or being positive for the ADT while the color of the bubble represents the average expression level. **D.** Epor transcript is expressed in only 10% of the classically-defined EBI macrophages in the combined Mac_c9 population (2 out of 18 from the saline-treated and 8 out of 83 from the Epo-treated mouse).

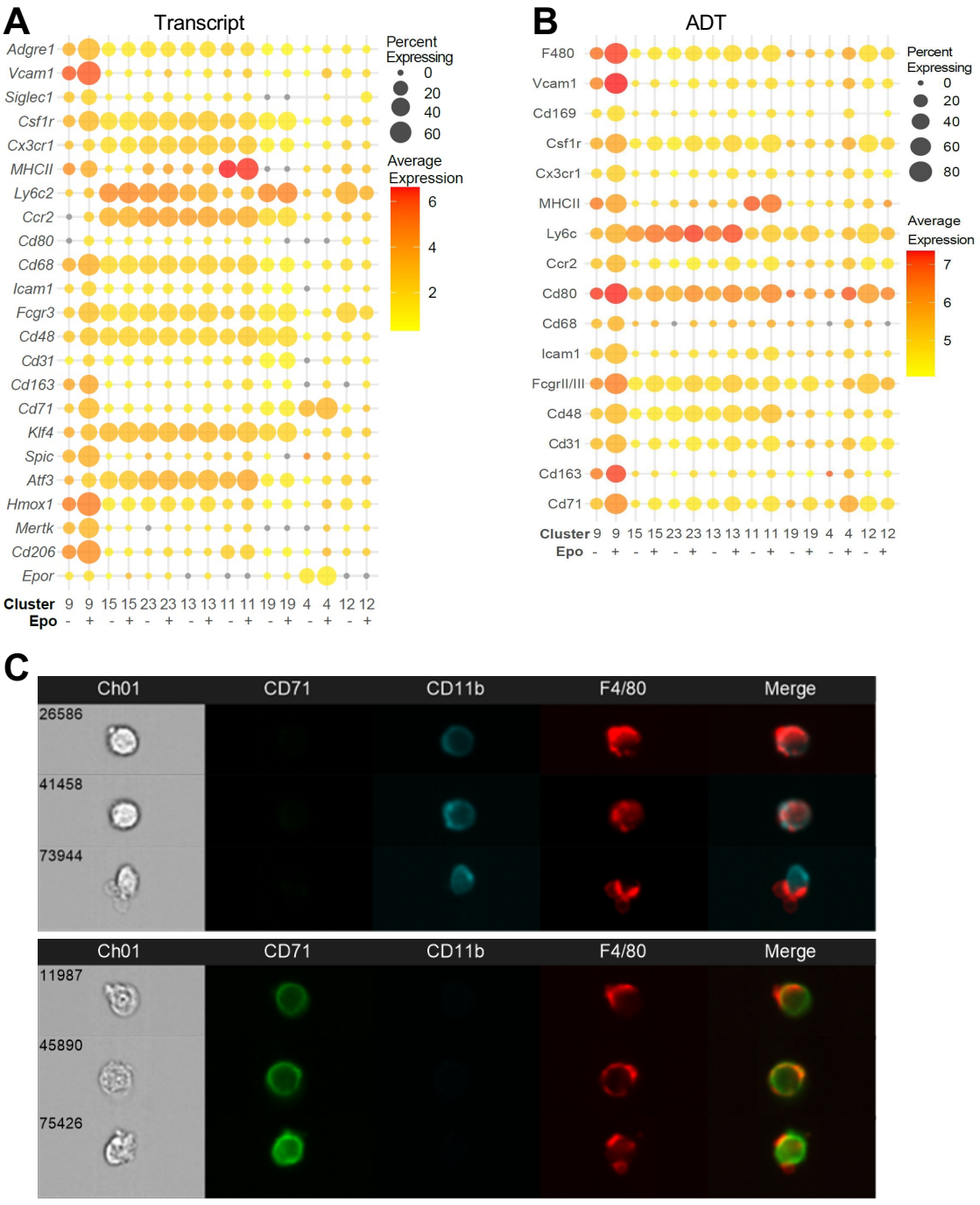

Supplemental Figure 8. Bubble plots show transcript and ADT levels in macrophage, erythroblast, and granulocytic precursors within the EBI. A and B. Bubble plots of mRNA **(A)** and ADTs **(B)** comparing classically defined EBI macrophage cluster 9 with the other macrophage/monocyte clusters in the CITE-seq capture, along with erythroid cluster 4 and the granulocyte cluster 12 for comparison. The size of the bubble indicates the percentage of cells from the total cells within the cluster, including both saline- and Epo treated samples, expressing the corresponding transcript or ADT and its relative proportion within the saline- or the Epo-treated sample. This representation demonstrates that each cluster is not exclusively comprised of either saline- or Epo- treated cells. If fewer than all cells of the cluster are positive for an ADT or transcript, then the size of the bubble decreases accordingly. The color of the bubble represents the average expression level. **C.** F4/80^{+} membrane fragments from macrophages on CD71^{+} and CD11b^{+} cells, indicating that macrophage specific epitopes can be detected on other cell populations, especially those previously associated within the EBI.

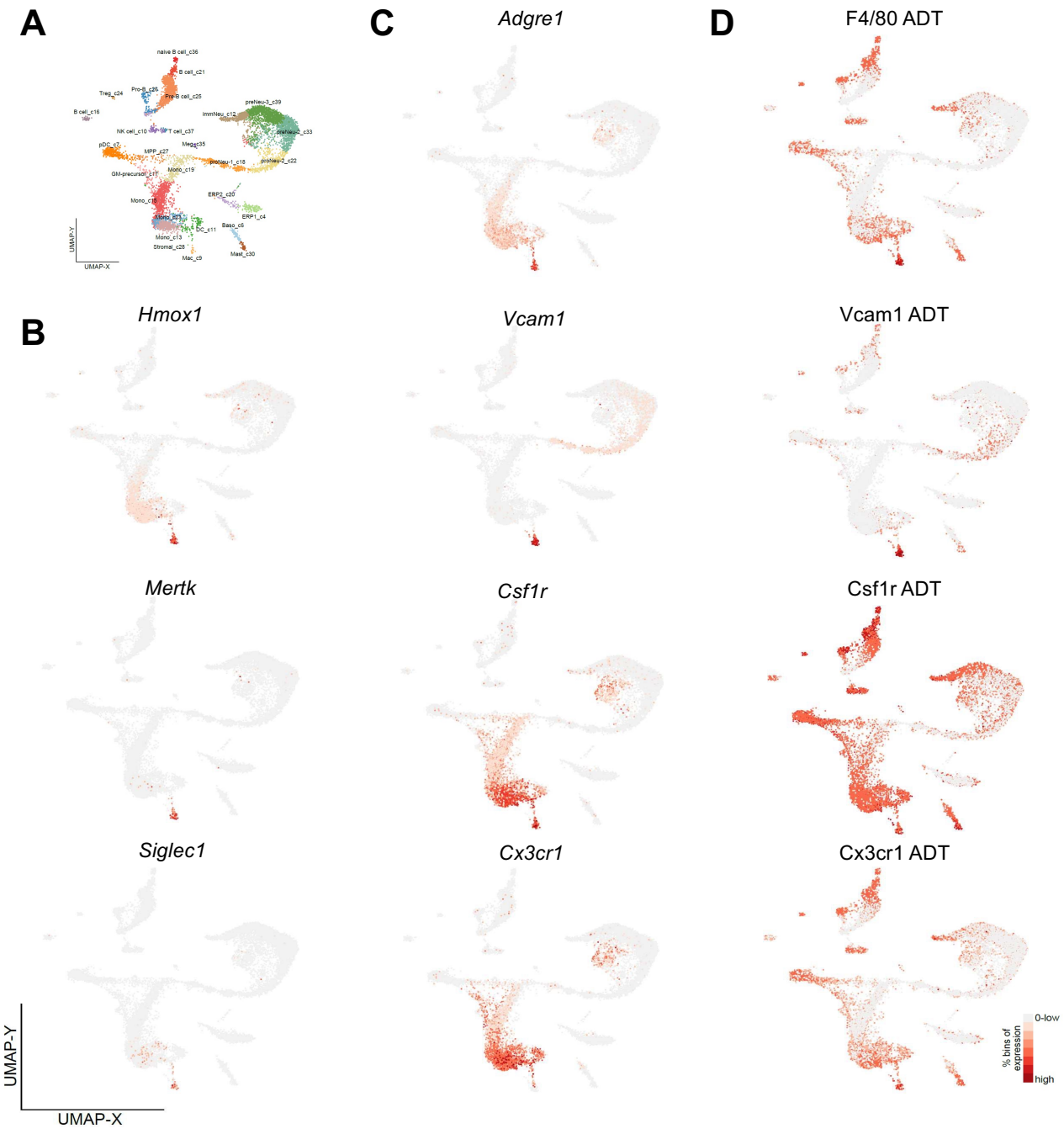

Supplemental Figure 9. Enrichment of EBI macrophages and other component cells for CITE-seq analysis. A. Heatmap of differentially expressed transcripts for the different cell groups captured by CITE-seq. Among the two erythroid populations remaining, we observe the predicted regulatory impact following Epo stimulation (Foxp3 versus Gata1 transcriptional repression), upregulated gene expression associated with heme biosynthesis and tubulin formation, and downregulated thrombin signaling, suggesting significant changes in the differentiation kinetics of erythroblast progenitors. **B.** Comprehensive differential expression analyses between Epo stimulated and controls using the software cellHarmony. **C.** EBI macrophages have both M1 and M2 characteristics. **D.** Epor transcript is heterogeneously observed at low levels within classically-defined EBI macrophages in Mac_c9.

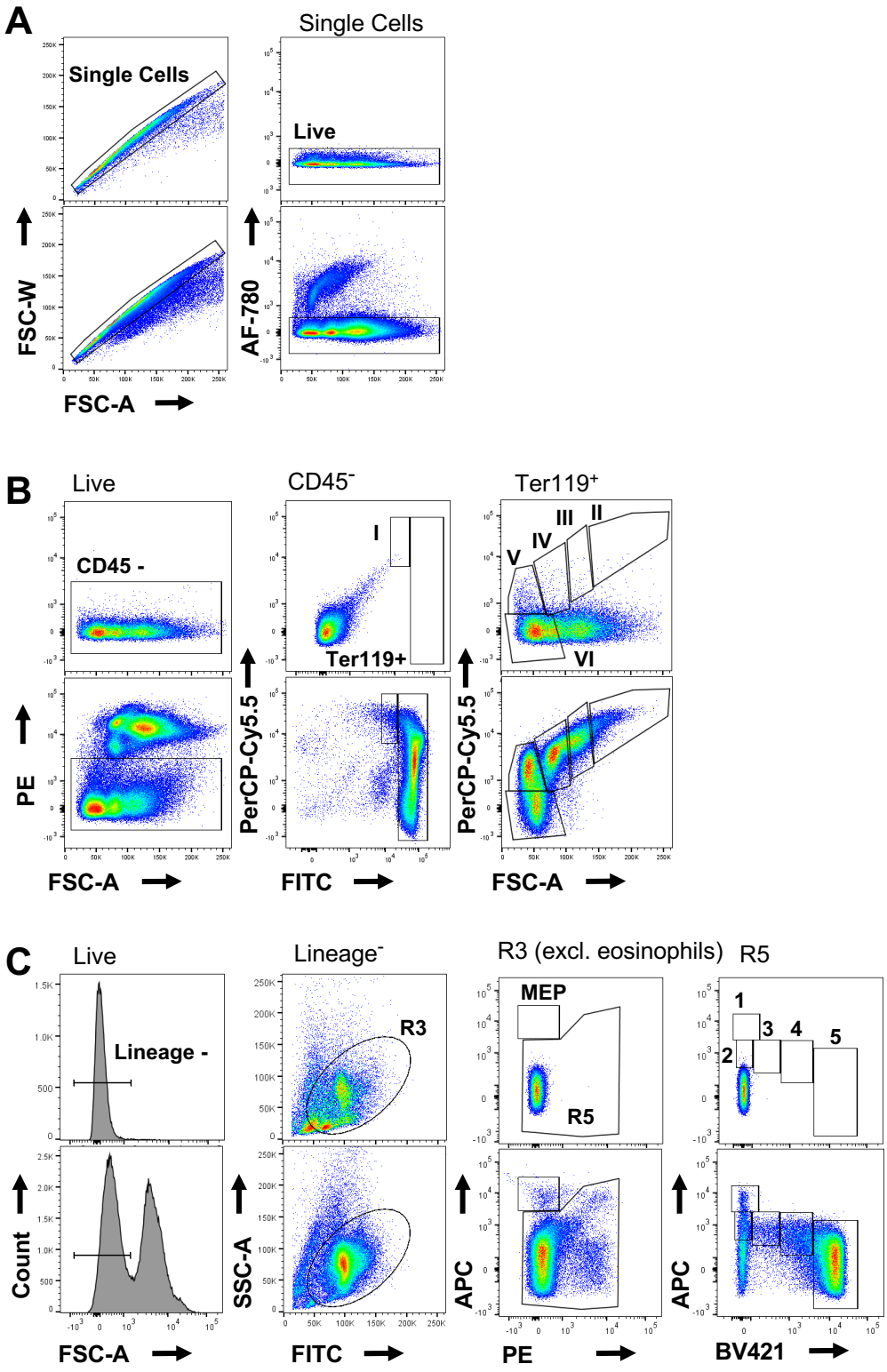

Supplemental Figure 10. Negative controls for flow cytometry. Unstained samples are used as control to establish gating. **A.** All flow cytometry events are gated on live, single cell events. **B.** Gating strategy for erythroblast evaluation and **C.** Gating strategy for granulocyte precursors evaluation by flow cytometry.